View metadata, citation and similar papers at core.ac.uk
brought to you by CORE
provided by UNT Digital Library

LAWRENCE
LIVERMORE
NATIONAL
LABORATORY

UCRL-PROC-227000

A multigroup radiation diffusion test problem: Comparison of code results with analytic solution

A. I. Shestakov, J. A. Harte, J. H. Bolstad, S. R. Offner

December 28, 2006

Nuclear Explosives Code Developers Conference
Los Alamos, NM, United States
October 22, 2006 through October 27, 2006

Disclaimer

This document was prepared as an account of work sponsored by an agency of the United States Government. Neither the United States Government nor the University of California nor any of their employees, makes any warranty, express or implied, or assumes any legal liability or responsibility for the accuracy, completeness, or usefulness of any information, apparatus, product, or process disclosed, or represents that its use would not infringe privately owned rights. Reference herein to any specific commercial product, process, or service by trade name, trademark, manufacturer, or otherwise, does not necessarily constitute or imply its endorsement, recommendation, or favoring by the United States Government or the University of California. The views and opinions of authors expressed herein do not necessarily state or reflect those of the United States Government or the University of California, and shall not be used for advertising or product endorsement purposes.

UCRL-CONF-223939

A multigroup radiation diffusion test problem: Comparison of code results with analytic solution*

Aleksei I. Shestakov, Judith A. Harte, John H. Bolstad
Lawrence Livermore National Laboratory
Livermore CA 94550

Stella S. R. Offner
Physics Dept., University of California
Berkeley CA 94720

Abstract

We consider a 1D, slab-symmetric test problem for the multigroup radiation diffusion and matter energy balance equations. The test simulates diffusion of energy from a hot central region. Opacities vary with the cube of the frequency and radiation emission is given by a Wien spectrum. We compare results from two LLNL codes, Raptor and Lasnex, with tabular data that define the analytic solution.

1 Introduction

This work stems from a test of the radiation multigroup (MG) diffusion scheme, recently developed by Shestakov and Offner [3], for the LLNL radiation hydrodynamic code Raptor. We consider a non-trivial test problem for the system coupling the multigroup diffusion and matter energy balance equations. The problem and its analytic solution was developed by Shestakov and Bolstad (S&B) [2]. We solve the problem with two LLNL codes, Raptor and Lasnex. Raptor is a massively parallel, multidimensional, Eulerian code with adaptive mesh refinement (AMR), while Lasnex is a well known design code for inertial confinement fusion research. Both code results are compared with tabular data that are more accurate than those published by S&B.

Validation and Verification (V&V) of code results is difficult for realistic multigroup problems since analytic solutions are either nonexistent or challenging to obtain. One then relies on the vagaries of code-to-code comparisons or

*This work was performed under the auspices of the U.S. Department of Energy by the University of California Lawrence Livermore National Laboratory under contract No. W-7405-Eng-48.

simply checks whether a result "looks right." Hence, it is fortunate to have an exact solution for a problem that captures the salient features of multigroup diffusion: frequency dependent opacities and radiation emission, inter-group coupling, etc. Such effects are inherent in the S&B test problems.

The S&B tables present results for a 64 group discretization of a linearized nondimensional set of multifrequency diffusion equations. The nonlinear nondimensional system was derived by Hald and Shestakov (H&S) [1]. In the following sections, we first review the derivation of the nonlinear nondimensional system. In Section 3, we discuss the linearization of the equations and the code modifications required to run the problem. In section 4, we describe the test problem, demonstrate its relevance to multigroup diffusion, compare Raptor and Lasnex results to tabular data, and lastly, show that Raptor's multigroup scheme's accuracy is first order in time and second order in space.

2 Derivation of nondimensional equations

The nonlinear multifrequency H&S system is derived by assuming slab symmetry, constant density, an ideal gas equation of state, and an opacity characteristic of free-free transitions. An advantage of the H&S system is its nondimensional form, which enables comparing results from codes using different dimensional units. For the codes we consider, Raptor uses CGS while Lasnex is in Jerk-shake (Jsh) units. In Jsh units, energy is in Jerk (10^{16} erg), time is in sh (10^{-8} s), photon frequency and temperatures are in keV, k (Jerk/keV) is the Boltzmann constant, and h (Jerk sh) is the Planck constant.

The H&S system is obtained using characteristic values for density ρ_0, temperature T_0, specific heat c_v, and inverse mean free path (mfp) $\kappa = \kappa_0/\nu^3$, where $\kappa_0 = \text{const}$ and ν is the frequency variable. Radiation emission is given by a Wien distribution $B = B_W$.[1] In CGS units, $B_W = B_0\,\nu^3 \exp(-h\nu/kT)$ where the constant,[2]

$$B_0 = 8\pi\, h/c^3 \,.$$

The inverse mfp appears in both the diffusion, $c/3\kappa$, and the radiation-matter coupling coefficients, $c\,\kappa$, where c is the speed of light. For this problem, the diffusion coefficient is *not* flux limited.

The normalization proceeds as follows. User-set parameters T_0, κ_0, ρ_0, and c_v define the required normalization constants. First, the characteristic frequency ν_0,

$$\nu_0 = k\,T_0/h \;\; \text{(CGS)} \;\; , \quad \nu_0 = T_0 \;\; \text{(Jsh)} \,.$$

[1]It is noteworthy that H&S's choice of opacity and Wien spectrum for B gives the same spectral radiation emission source $\kappa\, B_W$ as would be obtained by including stimulated emission (SE) effects [6] and letting B be the Planck function, since SE requires multiplying κ by the factor $(1 - e^{-h\nu/kT})$. Also note that without SE, the resulting Planck averaged gray opacity does not exist; the integral diverges.

[2]In Jsh units, $B_W = B_0\,\nu^3 \exp(-\nu/T)$, but with a different definition of B_0.

The rest of the normalization is almost the same for CGS or Jsh units. The frequency ν_0 defines a length ℓ_0 and the two lead to a normalization distance x_0, time t_0, spectral and total radiation energies u_0 and $E_{r,0}$:

$$\ell_0 = \nu_0^3/\kappa_0 \ , \quad x_0 = \ell_0/\sqrt{3} \ , \quad t_0 = \ell_0/c \ , \quad u_0 = B_0\, \nu_0^3 \ , \quad E_{r,0} = u_0\, \nu_0 \, .$$

By defining nondimensional variables, $x' = x/x_0$, $t' = t/t_0$, $\nu' = \nu/\nu_0$, $u' = u/u_0$, $T' = T/T_0$, (and dropping the primes) we obtain the normalized system,[3]

$$\partial_t u = \nabla \cdot \nu^3 \, \nabla u + (\nu^3 e^{-\nu/T} - u) \, / \, \nu^3 \, , \tag{1}$$

$$R \partial_t T = -T + \int_0^\infty (u/\nu^3) \, d\nu \, , \tag{2}$$

where the constant,

$$R = c_v \, \rho_0 \, h / u_0 \, k \ \ (\text{CGS}) \ \ , \quad R = c_v \, \rho_0 / u_0 \ \ (\text{Jsh}) \, . \tag{3}$$

Henceforth, unless stated otherwise, we use nondimensional variables.

The H&S system yields a precise definition of the multigroup equations since the integrals over groups can be computed exactly, an impossible task for definite integrals of the Planck function. Given a group structure $\{\nu_g\}_{g=0}^{G}$, after integrating over groups,

$$\partial_t u_g = \bar{\nu}_g^3 \partial_{xx} u_g + p_g \, T - u_g / \bar{\nu}_g^3 \, , \quad g = 1, \ldots, G \tag{4}$$

$$R \, \partial_t T = -T + \sum_{g=1}^{G} u_g / \bar{\nu}_g^3 \tag{5}$$

where $u_g = \int_g u \, d\nu$, and $\bar{\nu}_g$ is a group's representative frequency. S&B define $\bar{\nu}_g = \sqrt{\nu_{g-1} \nu_g}$ for $g = 2, \ldots, G$, and $\bar{\nu}_1 = \nu_1/2$ since the lowest group boundary $\nu_0 = 0$. The emission coefficients,

$$p_g \doteq \exp(-\nu_{g-1}/T) - \exp(-\nu_g/T) \, . \tag{6}$$

It is required that the group structure be sufficiently broad, i.e., that $\nu_0 = 0$ and $\nu_G/T \gg 1$ in order for $\sum_g p_g = 1$.

3 Linearization, code modification

Equations (4)–(5) are *nonlinear* because of the exponential dependence of $p_g(T)$. To obtain an analytic solution, S&B follow the approach of Su and Olson [4], [5], which requires a *linear* system since it uses Fourier and Laplace transforms.

[3] If instead of B_W, H&S had used the Planck function, the factor $e^{-\nu/T}$ in Eq. (1) would be replaced by $(e^{\nu/T} - 1)^{-1}$. However, H&S would then be unable to form Eq. (2), since the integral over all ν (the total emission) diverges—see prior footnote.

code	ρ_0 (g/cm^3)	T_0 (keV)	$\kappa_0{}^*$
Raptor	$1.8212111 \cdot 10^{-5}$	0.1	$4.0628337 \cdot 10^{43}$
Lasnex	1.0	1.0	1.0

Table 1: Code inputs. *Units of κ_0 Raptor: (cm^{-1} s^{-3}); Lasnex: (cm^{-1} keV^3).

S&B linearize (4)–(5) by defining an additional, fixed parameter T_f and substitute T_f for T in (6), i.e., $p_g(T) \to p_g(T_f)$.

Except for one item, it is easy to setup the S&B linearized MG system in a conventional rad-hydro code. Such codes usually allow an ideal gas equation of state and a desired analytic form for the opacity. One chooses *arbitrary* values for ρ_0, κ_0, T_0, and picks a specific heat c_v to set R. To prove our point, our simulations use the values in Table 1. In order to comply with the S&B specification, we chose c_v to obtain $R = 1$; see (3). Our ρ_0, T_0, and κ_0 choices were made solely by reasons of convenience. Since we compare with a nondimensional result, other values will also work.

The subtle item in setting up the problem is how to force a code's spectral emission rate to equal $p_g(T_f)\,T$. We accomplish the task as follows. In both Raptor and Lasnex, the gth group's radiation emission is linearized:

$$\kappa_g\, B_g(T) \to \kappa_g\, [B_g|_{T^*} + B_g'|_{T^*}\,(T - T^*)]\,.$$

The terms B_g and B_g' are integrals over the gth group, at temperature T^*, of the Planck function and its derivative with respect to T. The codes compute the integrals in a subroutine which takes T^* as an input variable. For the test problem, we use a different subroutine, which when called, first defines $B_g'|_{T^*} \propto \bar{\nu}_g^3\, p_g(T_f)$ and then sets

$$B_g = B_g'|_{T^*}\, T^*\,.$$

Specifically, for Raptor (CGS),

$$B_g' = (\bar{\nu}_g \nu_0)^3\,(8\pi k/c^3)\,[\exp(-y_{g-1}) - \exp(-y_g)\,]\,,$$

where $y_g = h\nu_g\nu_0/kT_fT_0$. In the definition of B_g', the terms ν_g and T_f are nondimensional, while ν_0 and T_0 are the normalization constants. The $(\bar{\nu}_g\nu_0)^3$ term cancels the opacity's $1/\nu^3$ dependence.

4 Test problem description

For the test, we consider S&B's problem 1, see [2]. The nondimensional domain is $0 < x < X$, where we set $X = 4$. The initial condition is $T = 1(0)$ for $x <$ $(>)\,0.5$ and $u = 0$ everywhere. We use symmetry boundary conditions at $x = 0$

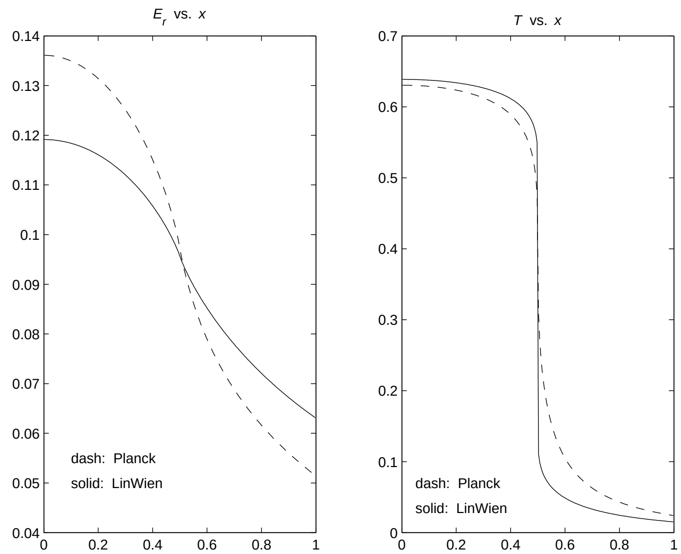

Figure 1: Comparison of the linear solution ($T_f = 1.0$) with the solution of the nonlinear MG system with Planckian emission; Raptor code; $t = 1$.

and homogeneous Milne at $x = X$. We use the same group structure as S&B: 64 groups, starting at zero, with widths increasing geometrically by a factor 1.1. We set $\nu_1 = 5.0 \cdot 10^{-4}$ as the width of the first group.[4] The test simulates an initially hot slab of matter encased by cold matter. Since u is initially zero throughout, the solution evolves by first coupling in the hot subdomain. As radiation diffuses out, it couples to cold matter thereby heating it. Because of the opacity's $1/\nu^3$ dependence, each group's diffusion and coupling rates differ.

4.1 Relevance of test problem

Although the problem appears contrived, we contend it is representative of radiation diffusion. We prove the assertion in Fig. 1 where we display the temperature T and the total radiation energy density E_r $(= \sum_g u_g)$ for two simulations ending at $t = 1$. Solid lines pertain to the linearized system, where $T_f = 1.0$. Dashed lines are solutions of the "physical" nonlinear MG system using Planckian emission. The similarity of the solutions validates the test problem. We used $T_f = 1.0$ in the simulation (instead of S&B's $T_f = 0.1$) because over the short duration of the simulation, the emission temperature in the hot subdomain is of order 1.0, rather than 0.1.

[4] A misprint in [2] erroneously has $\nu_1 = 10^{-4}$.

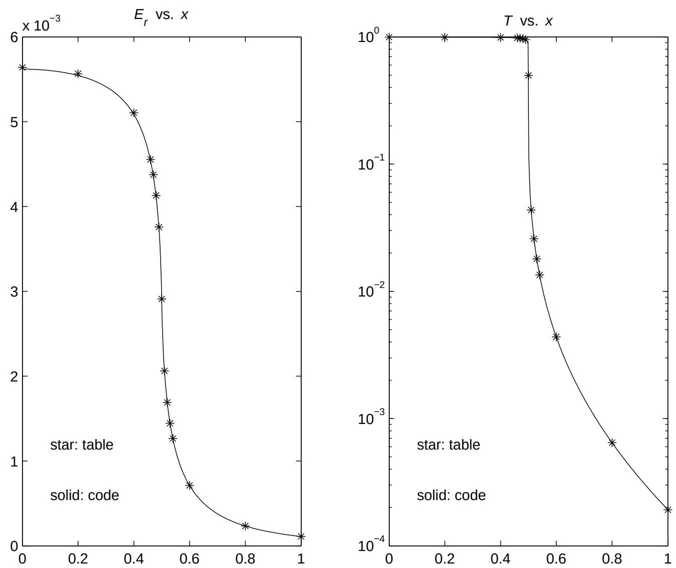

Figure 2: Comparison of Raptor's linear solution (solid lines, $T_f = 0.1$, $\Delta x = 0.0025$, $\Delta t = 0.5 \cdot 10^{-8}$ s) with the S&B tabular data (star symbols); $t = 1$.

4.2 Raptor, Lasnex results

We now present our MG result using S&B's parameter $T_f = 0.1$ and display the comparison to the analytic solution in Fig. 2. The near perfect overlay is a testament to the accuracy obtained by Raptor. For completeness, the tabular data at $t = 1.0$, which is more accurate than that published by S&B [2], is given in the appendix.

The tabular data allows us to get a better representation of the codes' accuracy by computing relative errors. We define the error $\varepsilon(f) \doteq |(\bar{f} - f_k)/\bar{f}|$, where f_k are the numerical results and $\bar{f}$ are the tabular data. Figure 3 displays the errors. Code results are obtained using a mesh size $h = 1/400$ and timestep $\Delta t = 1/200$. For completeness, the results of Fig. 3 are also listed in Table 2.

4.3 Raptor convergence

We conclude with a convergence study of Raptor's multigroup module.[5] We claim the scheme [3] is correct to first order in time and second order in space and prove the assertion using Richardson extrapolation. Let v_k denote a numerical solution to an equation discretized by a constant parameter k. For an initial-

[5]We focus attention on Raptor's module since it is well known that Lasnex's multigroup scheme is correct to second order in space and first order in time.

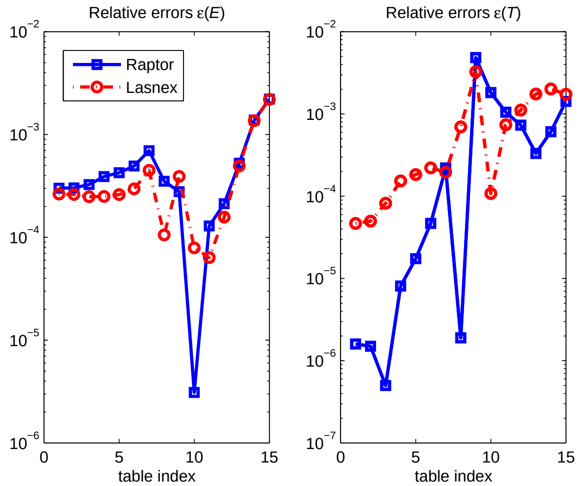

Figure 3: Linear MGD test. Raptor and Lasnex relative errors of temperature T (left graph) and radiation energy E_r (right graph); $T_f = 0.1$, $t = 1$.

x	$\varepsilon_R(T) \cdot 10^3$	$\varepsilon_L(T) \cdot 10^3$	$\varepsilon_R(E_r) \cdot 10^3$	$\varepsilon_L(E_r) \cdot 10^3$
0.00	0.0016	0.0467	0.3012	0.2637
0.20	0.0015	0.0498	0.3028	0.2612
0.40	0.0005	0.0822	0.3268	0.2489
0.46	0.0081	0.1537	0.3903	0.2498
0.47	0.0174	0.1834	0.4252	0.2611
0.48	0.0467	0.2217	0.4945	0.2968
0.49	0.2205	0.1960	0.6979	0.4500
0.50	0.0019	0.6982	0.3518	0.1058
0.51	4.8468	3.2595	0.2785	0.3915
0.52	1.8220	0.1080	0.0031	0.0791
0.53	1.0528	0.7390	0.1293	0.0635
0.54	0.7320	1.1184	0.2128	0.1574
0.60	0.3316	1.7494	0.5263	0.4961
0.80	0.6099	2.0155	1.3841	1.3675
1.00	1.4253	1.7345	2.2138	2.1985

Table 2: Linear MGD test; $T_f = 0.1$. Relative errors times 1000. Numerical results obtained using $h = 1/400$ and $\Delta t = 1/200$. Columns 2, 3 display temperature errors for Raptor, Lasnex resp. Columns 4, 5 display radiation energy errors (Raptor, Lasnex).

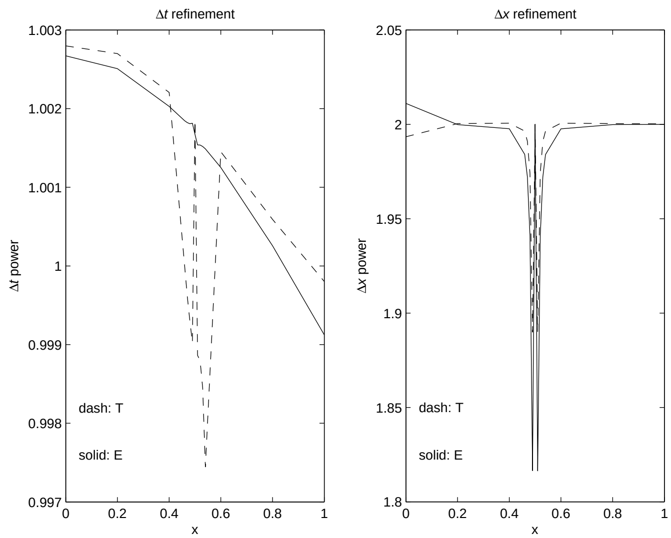

Figure 4: Timestep and meshsize orders of convergence; Δt (Δx) on left (right) sides; $t = 1.0$; see text.

value ODE, k denotes the timestep; for a time independent equation, k is the mesh width. If v is the analytic solution,

$$v_k = v + \alpha\, k^a + \mathcal{O}(k^b)\,,$$

where $0 < a < b$, and where α is independent of k. In the asymptotic regime, the k^a term dominates the error. Assuming we have three solutions v_k, v_{2k}, v_{4k}, we can combine v_k and v_{2k} to eliminate the k^a error. We can similarly combine v_k and v_{4k}. Setting the two combinations equal enables solving for the unknown order of convergence,

$$a = \left[\log\left(\frac{v_{2k} - v_{4k}}{v_k - v_{2k}}\right)\right] \Big/ \log 2\,.$$

We apply this procedure to estimate the orders of convergence. First, for the Δt study, we fix $h = 0.01$ and obtain three results using $k = 0.5 \cdot 10^{-8}$ s, $2k$ and $4k$. For the Δx study, we fix $\Delta t = 0.5 \cdot 10^{-8}$ s and use $k = 0.0025$. In both studies, runs are halted when $t = t_0$, i.e., $t = 1$ in nondimensional units. We compute a at 15 points across the domain $(0,\, 1)$ for both E_r and T and focus attention at $x = 0.5$, where the fields undergo the sharpest change. Results are presented in Fig. 4. The left plot clearly displays first order temporal convergence since $a \approx 1$ across the domain. The right plot supports our claim of second order spatial convergence. The low $a \approx 1.82$ (1.89) values for E_r (T) arise only at the two points $x = 0.49,\, 0.51$. It appears that at these points, we are not yet in the asymptotic regime.

4.4 Conclusion

To summarize, we have shown: (1) With a proper choice of T_f, the test problem closely resembles MG physics. (2) Raptor and Lasnex show excellent agreement with the analytic solution. (3) Raptor's scheme is correct to first order in time and second order in space.

References

[1] O. H. Hald and A. I. Shestakov, "Stability of stationary solutions of the multifrequency radiation diffusion equations," *SIAM J. Appl. Math.*, **65**, 1, 175–193 (2004).

[2] A. I. Shestakov and J. H. Bolstad, "An exact solution for the linearized multifrequency radiation diffusion equation," *J. Quant. Spectrosc. Radiat. Transfer,* **91**, 2, 133–153 (2005).

[3] A. I. Shestakov and S. S. R. Offner, "A multigroup diffusion solver using pseudo transient continuation for a radiation- hydrodynamic code with patch-based AMR," Lawrence Livermore National Laboratory Report UCRL-JRNL-224845 (2006), submitted to *J. Comp. Phys.*

[4] B. Su and G. L. Olson, "Non-grey benchmark results for two temperature non-equilibrium radiative transfer," *J. Quant. Spec. Rad. Trans.,* **62** 279–302 (1999).

[5] B. Su and G. L. Olson, "An analytical benchmark for non-equilibrium radiative transfer in an isotropically scattering medium,," *Ann. Nucl. Energy,* **24**, 13 1035–1055 (1997).

[6] Ya. B. Zel'dovich and Yu. P. Raizer, *Physics of Shock Waves and High-Temperature Hydrodynamic Phenomena*, Dover 0-486-42002-7 (2001).

A Table

x	T	E_r	$\epsilon(T)$	$\epsilon(E_r)$
0.0E+00	9.9373253E-01	5.6401674E-03	5.4E-09	5.9E-11
2.0E-01	9.9339523E-01	5.5646351E-03	1.8E-08	7.0E-11
4.0E-01	9.8969664E-01	5.1047352E-03	6.0E-09	6.2E-11
4.6E-01	9.8060848E-01	4.5542134E-03	9.8E-09	6.4E-11
4.7E-01	9.7609654E-01	4.3744933E-03	1.3E-08	6.9E-11
4.8E-01	9.6819424E-01	4.1294850E-03	8.2E-09	6.3E-11
4.9E-01	9.5044751E-01	3.7570008E-03	6.7E-09	6.3E-11
5.0E-01	4.9704000E-01	2.9096931E-03	7.7E-09	2.8E-11
5.1E-01	4.3632445E-02	2.0623647E-03	1.2E-08	6.3E-11
5.2E-01	2.5885608E-02	1.6898183E-03	1.3E-08	6.3E-11
5.3E-01	1.7983134E-02	1.4447063E-03	1.8E-08	7.0E-11
5.4E-01	1.3470947E-02	1.2648409E-03	1.5E-08	6.5E-11
6.0E-01	4.3797848E-03	7.1255738E-04	1.1E-08	6.4E-11
8.0E-01	6.4654865E-04	2.3412650E-04	2.3E-08	6.8E-11
1.0E+00	1.9181546E-04	1.0934921E-04	1.0E-08	6.1E-11

Table 3: Analytic solution of test problem. Time $t = 1.0$, $T_f = 0.1$. Columns 4 and 5 give maximum absolute error estimates. Hence, at $x = 0$, entry T is correct to ±5.4E-09, i.e., has 8 trustworthy digits.